Identification of a Novel Domain of Fibroblast Growth Factor 2 Controlling Its Angiogenic Properties*

Antonio Facchiano‡§, Katia Russo‡, Angelo M. Facchiano¶, Francesco De Marchis‡, Francesco Facchiano‡, Domenico Ribatti‖, Maria S. Aguzzi‡, and Maurizio C. Capogrossi‡

From the ‡Laboratorio Patologia Vascolare, Istituto Dermopatico dell'Immacolata, IRCCS, 00167 Roma, Italy, the ¶Laboratorio di Bioinformatica e Biologia Computazionale, Istituto Scienze dell'Alimentazione, CNR, 83100 Avellino, Italy, and the ‖Dipartimento Anatomia Umana e Istologia, Università degli Studi di Bari, 70124 Bari, Italy

Fibroblast growth factor 2 (FGF-2) is a potent factor modulating the activity of many cell types. Its dimerization and binding to high affinity receptors are considered to be necessary steps to induce FGF receptor phosphorylation and signaling activation. A structural analysis was carried out and a region encompassing residues 48–58 of human FGF-2 was identified, as potentially involved in FGF-2 dimerization. A peptide (FREG-48–58) derived from this region strongly and specifically inhibited FGF-2 induced proliferation and migration of primary bovine aorta endothelial cells (BAEC) *in vitro*, and markedly reduced FGF-2-dependent angiogenesis in two distinct *in vivo* assays. To further investigate the role of region 48–58, a polyclonal antibody raised against FREG-(48–58) was tested and was found to block FGF-2 action *in vitro*. Human FGF-2 has three histidine residues, one falling within the region 48–58. Chemical modification of histidine residues blocked FGF-2 activity and FREG-(48–58) inhibitory effect *in vitro*, indicating that histidine residues, in particular the one within FREG-(48–58) region, play a crucial role in the observed activity. Additional experiments showed that FREG-(48–58) specifically interacted with FGF-2, impaired FGF-2-interaction with itself, with heparin and with FGF receptor 1, and inhibited FGF-2-induced receptor phosphorylation and FGF-2 internalization. These data indicate for the first time that region 48–58 of FGF-2 is a functional domain controlling FGF-2 activity.

Fibroblast growth factor 2 (FGF-2)[1] belongs to the fibroblast growth factor family and is one of the most potent growth factors regulating cellular functions including proliferation and chemotaxis, tissue and organ development, and tissue repair (1–3). FGF-2 has been suggested to play a key role in the etiology and progression of several pathological conditions including Parkinson's and Alzheimer's diseases (4–5), tumor growth and progression (6–9), atherosclerosis, and restenosis after angioplasty (10). A specific role has been indicated for FGF-2 in tumor angiogenesis (11–12) and in neuronal differentiation (13–14).

In light of the key role FGF-2 plays in both physiologic and pathologic conditions, structural-functional relationships studies on this factor are of large interest. FGF-2 dimerization and its interaction with heparan sulfates are necessary steps required for binding to high affinity receptors and for the following signaling activation. Several reports investigated functionally relevant regions of FGF-2 by analyzing crystallographic structures or by mutagenesis studies. FGF-2 dimer has not been crystallized, and different studies based on molecular simulations indicated different regions possibly lying at the FGF-2 dimer interface (15–17), whereas crystallization (18–20) and other studies (21–26) identified residues crucial for FGF-2 activity and involved in the interaction with heparin and high affinity receptors. Finally, specific residues were found to control the FGF-2 ability to induce production of urokinase-type plasminogen activator, likely in the FGF-2 nuclear localization site (27–28).

Despite all ongoing investigations, a specific site regulating the whole FGF-2 activity by controlling FGF-2 interaction with itself, has not yet been identified. We recently showed that FGF-2 directly interacts with PDGF-BB (29–30), leading to a marked inhibition of its angiogenic properties *in vitro* and *in vivo* (31). In the present study we report the novel identification of an FGF-2 functional domain controlling *in vitro* and *in vivo* FGF-2 properties, likely by controlling dimer formation.

EXPERIMENTAL PROCEDURES

Structural Analysis of FGF-2, Active Site Identification, and Peptide Synthesis

FGF-2 sequences were retrieved from the Web site of the National Library of Medicine (www.ncbi.nlm.nih.gov) and aligned by using ClustalW software (32). Accession numbers are reported in the legend of Fig. 1. Three-dimensional analysis was carried out on two high-resolution crystallographic structures from the Protein Data Bank (PDB), *i.e.* 2FBH and 1FQ9 for FGF-2 and the FGF-2/FGFR-1/heparin complex, respectively. Solvent accessibility analysis was performed using NACCESS software (33) to identify FGF-2 regions interacting with FGF-R1, according to a procedure previously used (17, 29). Solvent accessibility of each amino acid was evaluated for FGF-2 alone and for receptor-bound FGF-2; amino acids undergoing a marked accessibility modification within the complex were assigned at the ligand-receptor interface. FGF-2 secondary structure was evaluated by analyzing 2FBH molecular co-ordinates with DSSP software (34). Regions potentially falling at the FGF-2 dimerization sites were predicted by molecular docking simulations performed with GRAMM software (35, 36), through a procedure used for both high- (37, 38) and low-resolution (29, 39) simulations. In this study low-resolution docking parameters for globular proteins were used according to the GRAMM software manual.

[1] The abbreviations used are: FGF-2, fibroblast growth factor 2; PDGF-BB, platelet-derived growth factor-BB; FREG-(48–58), FGF-2 region 48–58; SCR, two scrambled versions of FREG-(48–58); VEGF, vascular endothelial growth factor; EGF, epidermal growth factor; BSA, bovine serum albumin; DEPC, diethylpyrocarbonate; SPR, surface plasmon resonance; PBS, phosphate-buffered saline; BAEC, primary bovine aorta endothelial cells; CAM, chick embryo chorioallantoic membrane; RU, resonance units; PDB, protein data bank.
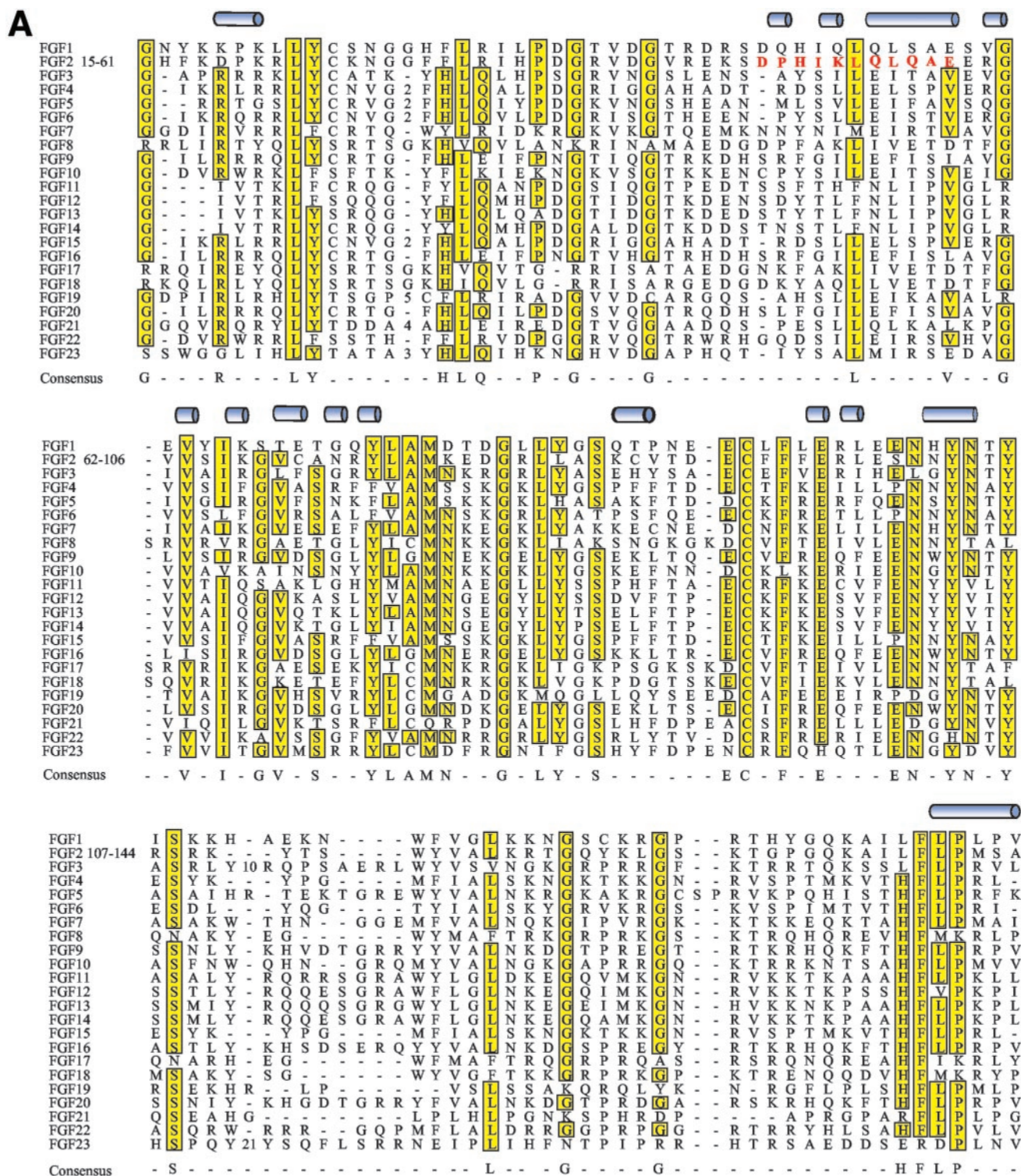
FIG. 1. **Sequence alignment and structure analysis.** *A,* FGF family alignment. Sequence alignment of 23 FGFs (all human, except FGF 15, of unknown source) was achieved by ClustalW software available at emb1.bcc.univie.ac.at/embnet/progs/clustal/. FGFs accession numbers are: FGF1, XP_054732; FGF2, XP_054784; FGF3, NP_005238; FGF4, XP_053627; FGF5, P12034; FGF6, P10767; FGF7, XP_017651; FGF8, BAA28605; FGF9, NP_002001; FGF10, NP_004456; FGF11, AAL15439; FGF12, XP_003135; FGF13isoform 1A, NP_004105; FGF14, NP_004106; FGF15, AR015075; FGF16, NP_003859; FGF17, NP_003858; FGF18, NP_387498; FGF19, AAH17664; FGF20, NP_062825; FGF21, NP_061986; FGF22, NP_065688; FGF23, NP_065689. The alignment is reported for the FGF-2 portion whose crystallographic coordinates are available. The consensus sequence at 60% identity level is reported (*boxed* residues on *yellow* background). FREG-(48–58) is indicated in *red*. *Blue cylinders* indicate regions predicted to be involved in FGF-2 dimerization according to the predicted dimer reported in *panel B*. Residues interacting with the receptor, identified according to solvent accessibility analysis on the PDB structure 1FQ9 (20), were: His-16, Phe-17, Lys-18, Lys-21, Tyr-24, Lys-26, Gly-28, Gly-29, Phe-31, Arg-44, Lys-46, Gln-54, Leu-55, Gln-56, Ala-57, Gln-58, Glu-59, Arg-60, Gly-61, Val-63, Ser-64, Tyr-73, Val-88, Glu-96, Arg-97, Leu-98, Glu-99, Ser-100, Asn-101, Asn-102, Tyr-103, Asn-104, Gly-131, Pro-132, Gly-133, Gln-134, Lys-135, Leu-138, Leu-140, Pro-141. Predicted dimerization sites and observed receptor-interacting residues partially overlap in the FREG-(48–58) region. Gaps longer than two positions were reported as the number indicating the gap length. *B,* docking simulation of two FGF-2 monomers (PDB code: 2BFH) achieved with GRAMM software. The two chains are colored in *blue* and *green; red* segments correspond to residues 48–58 selected to designate FREG-(48–58) and appear to be at the dimer interface.

B

Asp48   Glu58
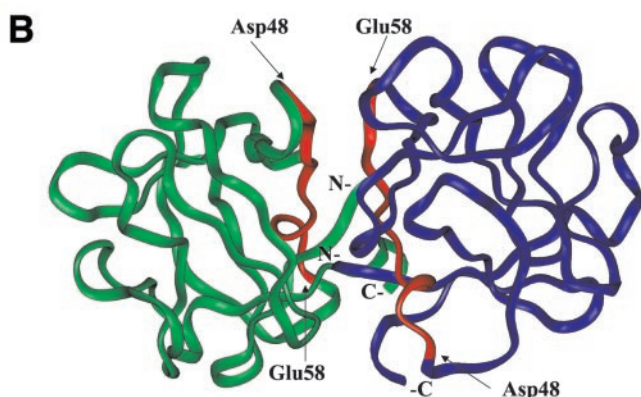
N-

N-

C-

Glu58   -C   Asp48

FIG. 1—*continued*

Regions at the interface of the predicted FGF-2 dimer were identified by solvent accessibility analysis as described above. According to these analyses, the FGF-2 region including the sequence DPHIKLQLQAE (here referred to as FREG-(48–58)) was identified. FREG-(48–58) was then custom synthesized by Research Genetics Inc. As a sequence-specificity control, two different scrambled versions of FREG-(48–58) (KHIAQLDEPLQ and KLQLDIEAHPQ), were synthesized by Neosystem Laboratoire. They are here referred to as SCR. Peptide purity, assessed by reverse-phase HPLC and mass spectrometry, was higher than 95% in all cases. Different batches of FREG-(48–58) and SCR gave similar results in all biological assays.

Cell Isolation and Cell Culture

BAEC were derived from adult bovine aorta and cultured as previously reported (40). Cell purity was evaluated by DiI-Ac-LDL uptake and was consistently >97%. BAEC at passage 3–7 and at 80% confluence were used in all assays.

Proliferation and Migration Assays

Proliferation assays were carried out as previously reported (31). After 24 h of starvation, BAEC were incubated with Dulbecco's modified Eagle's medium-BSA (0.1%) alone or containing human recombinant growth factors (10 ng/ml) as reported, in the absence or in the presence of FREG-(48–58) or SCR, the antibody raised against FREG-(48–58) (AbFREG-(48–58)), or preimmune control serum (AbP-I). BSA fraction V (Sigma) was used throughout the study. Time course experiments were carried out at 1-, 2-, and 3-day time points at 10 ng/ml FREG-(48–58) concentration. Cells were then harvested and counted with a hemacytometer. The FREG-(48–58) dose used in most experiments (*i.e.* 10 ng/ml) was identified in dose dependence tests carried out in cell proliferation and receptor phosphorylation experiments.

Migration assays were carried out in modified Boyden chambers (Costar Scientific Corporation) as previously reported (31). Briefly, BAEC seeded on gelatin-coated polycarbonate filters (12-μm pores) (Costar) were exposed to FGF-2 (Invitrogen), vascular endothelial growth factor (VEGF) (RnD Systems), epidermal growth factor (EGF) (Invitrogen), or fibronectin (Invitrogen) human recombinant factors, dissolved at the reported concentration in Dulbecco's modified Eagle's medium, 0.1% BSA. FREG-(48–58) or SCR were supplemented to the growth factor solution at the reported final concentration. Assays were carried out at 37 °C in 5% CO_2, for 6 h. Migrated cells were counted at $\times$400 magnification in 15 fields for each filter, and the average number $\pm$ S.D. of cells/field was reported. All experiments were performed at least three times in duplicate.

Histidine Residue Chemical Modification

Chemical modification of histidine residues was achieved by diethylpyrocarbonate (DEPC) treatment, which specifically modifies the imidazolic ring of histidine residues (41). Briefly, an aliquot of a freshly prepared DEPC solution (Sigma) in anhydrous ethanol was added to FGF-2 in PBS, to reach 200 μM DEPC and 55 μM FGF-2 final concentration. After 15 min at 25 °C the reaction was stopped with 100 mM Tris-HCl (pH 7.6). DEPC-induced modification of FREG-(48–58) was carried out similarly. In control experiments DEPC was first inactivated by prior incubation with 100 mM Tris-HCl, and then added to the sample. Histidine-modified FREG-(48–58) and FGF-2 were then tested in SPR (see below) and migration assays.

Peptide and FGF-2 Biotinylation

Biotinylation was carried out according to the manufacturer's instructions (Pierce). Briefly, FREG-(48–58) (2 mg/ml) or FGF-2 (20 μg/ml) in PBS (500 μl) (pH 7.4) were incubated with 2 mM EZ-Linksulfo-NHS-biotin (Pierce) for 30 min at room temperature to label amines. The excess reagent was quenched by incubation with 100 mM Tris-HCl (pH 7.4) for 15 min at room temperature. The mixture was then dialyzed against PBS; biotinylated FREG-(48–58) was then immediately used in an overlay assay, and biotinylated FGF-2 was immediately used in internalization assays.

Fluorescence Analysis

Fluorescence spectroscopy experiments were carried out as previously reported with modifications (29, 42) on a Perkin Elmer LS55 fluorimeter at constant temperature (22 °C). Briefly, 10 aliquots (0.5 μl each) of FREG-(48–58) or SCR (85 μM, 0.1 mg/ml in PBS) were subsequently added to 90 μl of FGF-2 in PBS (2 μM, 36 μg/ml). Under these conditions, the FGF-2 sample reached only 5% dilution. Fluorescence emission spectra were collected by excitation at 277 nm. Peak fluorescence was at 310 nm as previously reported for similar experimental conditions (43). Data were corrected for the buffer, FREG-(48–58), and SCR contributions and for the dilution factor, and its value was plotted as a function of the amount of peptide supplemented. Data were analyzed according to the single site tight binding model (44).

FGF-2 Interaction with FGF-2, with Heparin, or with FGF Receptor 1 by Surface Plasmon Resonance (SPR) Analysis

SPR experiments were carried out as previously reported (29, 45) on the BIAcoreX instrument (Amersham Biosciences Biosensor AB).

Immobilization—FGF-2 or recombinant human FGF-R1β (IIIC)/FC chimera (RnD Systems) were covalently coupled to the CM5 sensor chip by injecting FGF-2 or FGF-R1 (80 μl, 1.25 μg/ml and 55.5 μg/ml, respectively) dissolved in 30 mM acetate buffer, pH 4.8. Immobilized FGF-2 and FGF-R1 achieved about 500 and 7500 Resonance Units (RU), respectively, corresponding approximately to 0.5 and 7.5 ng/mm^2, respectively (46). Immobilized FGF-2 was recognized by injecting a goat anti-human FGF-2 antibody (RnD Systems). All experiments were performed using HBS (10 mM Hepes, 0.15 M NaCl, 3 mM EDTA, 0.005% (v/v) surfactant P20, pH 7.4) as running buffer and as a dilution buffer for FGF-2. In additional experiments, biotinylated low molecular weight heparin (2.6 mg/ml in HBS containing 0.3 M NaCl, 30 μl) was captured onto a BIAcore SA chip (carrying streptavidin on the surface) via biotin-streptavidin interaction at a 5 μl/min flow rate. Under these conditions immobilized heparin reached about 200 RU.

Injection—FGF-2 (20 μl, 1.25 μg/ml) was injected for a 2-min association phase with or without increasing concentrations of FREG-(48–58) or SCR, followed by HBS flow for a 30-s dissociation phase. Response, monitored at 25 °C, was expressed in RU. Sensor chip regeneration was achieved by NaOH injections (50 mM, 10 μl each). A 10 μl/min flow rate was used throughout the experiments.

Overlay Experiments

Either FGF-2 or BSA (300 ng) were spotted onto a nitrocellulose membrane as previously reported (29), then blocked with 5% dry milk (Bio-Rad) in TPBS (0.1% Tween 20 in PBS). In addition to BSA, an additional control was introduced, corresponding to the mix of molecular weight standards (Amersham Biosciences) listed in the legend of Fig. 4. After the TPBS wash, the membrane was incubated with biotinylated FREG-(48–58) (2 ml, 200 μg/ml) for 4 h at room temperature and washed again. Interaction was detected by an avidin/biotinylated horseradish peroxidase kit (Vectstain ABC, from Vector) followed by chemiluminescent reaction and exposure to Kodak film (Eastman Kodak).

FGF-2 Internalization

FGF-2 internalization was measured as described (47). BAEC (5 $\times$ 10^5) were incubated with biotinylated FGF-2 (10 ng/ml) alone or in the presence of either FREG-(48–58) (20 ng/ml), SCR (20 ng/ml), mAb 125 (monoclonal antibody neutralizing FGF-2 receptor, Chemicon) (500 ng/ml), rabbit AbFREG48–58 (1:200 dilution), or rabbit preimmune serum (AbP-I) (1:200) at 37 °C in a 5% CO_2 atmosphere. After 1 h, cells were washed and cell surface-bound material was extracted by washing with 2 M NaCl in 20 mM Hepes buffer (pH 7.4) and with 2 M NaCl in 20 mM acetic acid (pH 4.0) and discarded. Cells were then lysed with lysis buffer containing 20 mM Tris-HCl, pH 7.5, 150 mM NaCl, 1 mM EDTA, 1 mM EGTA, 1% Triton X-100, 2.5 mM sodium pyrophosphate, 1 mM β-glycerol phosphate, 1 mM Na_3VO_4, 1 μg/ml leupeptin, and 1 mM phenylmethylsulfonyl fluoride (Sigma), and the total lysate was immo-
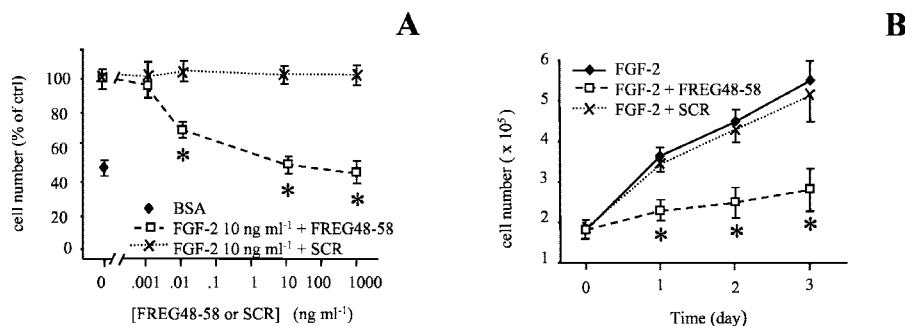
FIG. 2. **BAEC proliferation.** *A*, FREG-(48–58) effect on FGF-2-induced BAEC proliferation. Cells were incubated for 48 h with FGF-2 (10 ng/ml) in Dulbecco's modified Eagle's medium, BSA (0.1%) alone or in the presence of increasing doses of either FREG-(48–58) or SCR. Results are expressed as average percent of cell number *versus* cells treated with FGF-2 only ± S.D. Absolute value corresponding to 100% is 9.5×10^5 cells. Experiments were performed four times in duplicate. *Asterisks* indicate $p < 0.01$ *versus* FGF-2 alone. *B*, time course experiments on BAEC proliferation. BAEC were incubated with FGF-2 (10 ng/ml) alone or in the presence of FREG-(48–58) or SCR (10 ng/ml) up to 3 days. FREG-(48–58) was added at time 0 and time 48 h. Results are expressed as average cell number ± S.D. Experiments were performed three times in duplicate. *Asterisks* indicate $p < 0.01$ *versus* time 0.

FIG. 3. **BAEC migration.** Effect of FREG-(48–58) and SCR (10 ng/ml) on FGF-2-induced (*A*), EGF-induced (*B*), fibronectin-induced (*C*), and VEGF-induced (*D*) BAEC migration. FREG-(48–58) showed a significant inhibitory effect on FGF-2 only, while SCR was inactive in all cases. *Asterisk* indicates $p < 0.01$ *versus* FGF-2 alone.
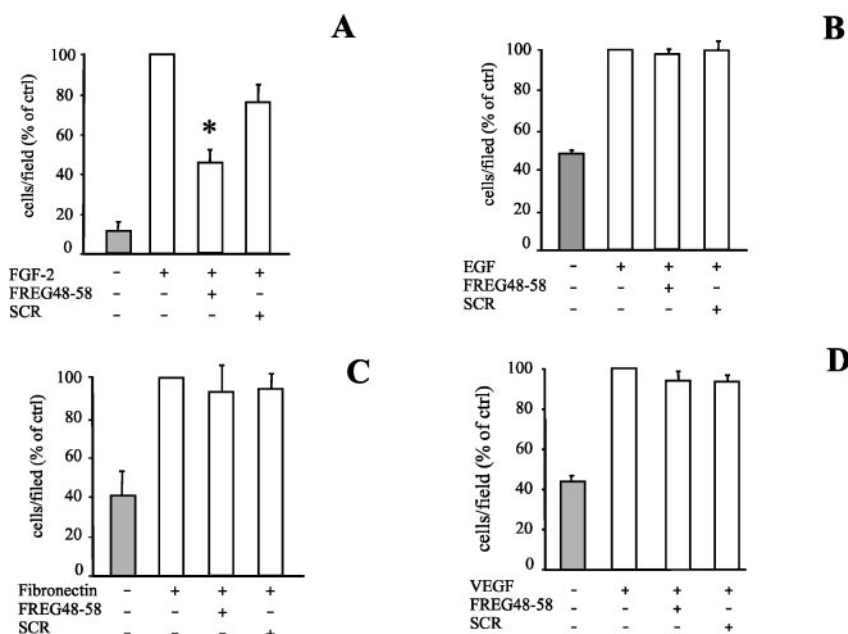
bilized onto nitrocellulose and blocked with 5% dry milk in TPBS. After washing with TPBS, biotinylated FGF-2 was then revealed with the Vectstain ABC Kit as in overlay experiments. The film was then subjected to densitometry analysis (GS 710, Bio-Rad).

FGF-R1 Phosphorylation

After 24 h of starvation, BAEC were incubated with FGF-2 (10 ng/ml) diluted in 0.1% BSA, in the absence or in the presence of FREG-(48–58) or SCR (10 ng/ml) for 10 min. Cells were then washed in ice-cold PBS and scraped with lysis buffer (as above). Cell extracts were sonicated and centrifuged, and supernatants were collected. Immunoprecipitation was then carried out on samples (60 µg of protein) by incubating with anti-FGF receptor antibody (mAb 125, Chemicon) (2 µg) at 4 °C overnight on a rocking bath, followed by incubation with 10 µg of protein G-Sepharose 4 Fast Flow (Amersham Biosciences) for 2 h at 4 °C. After washing with lysis buffer, complexes were dissolved in Laemmli buffer, separated by 8% SDS-PAGE, blotted onto nitrocellulose membrane, blocked as reported above, incubated with a monoclonal anti-phosphotyrosine antibody (clone PT66, Sigma) (1:2000 dilution) for 1 h at room temperature, revealed by chemiluminescence (Amersham Biosciences), and quantified by densitometry.

Production and Testing of the Rabbit Anti-FREG-(48–58) Antibody (AbFREG48–58)

Antibody against FREG-(48–58) (AbFREG48–58) was developed according to standard protocols. Briefly, FREG-(48–58) (1 mg) dissolved in 2 ml of PBS and supplemented with Complete Freund's Adjuvant, was administered by intramuscular injection in two 5-month-old New

Zealand rabbits. After 22 and 44 days the antigen injection was repeated with un-complete Freund's Adjuvant. Fifteen days after the third injection, blood was collected, and the serum was separated and stored at −20 °C in aliquots. Before some experiments, rabbit serum was collected after four antigen injections and showed activity at a higher dilution. The ability of this antibody to recognize the whole FGF-2 was tested by spotting increasing quantities of FGF-2 (up to 100 ng/spot) onto nitrocellulose membranes and then blocking with 5% dry milk. After TPBS washing, membranes were incubated with AbFREG48–58 (1:200 in PBS) for 1 h at room temperature. Membranes were then washed and incubated with anti-rabbit peroxidase-conjugated IgG (Pierce) for 1 h at room temperature; detection was achieved by chemiluminescence (Amersham Biosciences). FREG-(48–58) up to 100 ng/ml was used to compete for the observed interaction between FGF-2 and AbFREG48–58. AbFREG48–58 was then used in internalization and proliferation assays as reported.

In Vivo Angiogenesis Assays

Procedures involving animals and their care were conducted according to the institutional guidelines, in compliance with international laws and policies (Guide for the Care and Use of Laboratory Animals; United States National Research Council, 1996).

Angiogenesis in Chick Embryo Chorioallantoic Membrane (CAM Assay)

CAM assays were performed as previously reported (31). Fertilized White Leghorn chicken eggs (10/group) were incubated at 37 °C at constant humidity. On incubation day 3, 2 ml of albumin were removed

FIG. 4. **FREG-(48–58) interacting properties.** *A*, overlay assay of biotinylated FREG-(48–58) on immobilized FGF-2. Biotinylated FREG-(48–58) interacted with FGF-2 immobilized onto nitrocellulose (300 ng/spot), whereas no interaction was observed with immobilized BSA (300 ng/spot) or with immobilized molecular weight standards (Amersham Biosciences, 300 ng/spot) (Mix) consisting of a mixture of myosin, phosphorylase B, BSA, ovalbumin, carbonic anhydrase, trypsin inhibitor, and lysozyme. A representative experiment is shown. This experiment was performed three times with similar results. *B*, fluorescence spectra of FGF-2 (2 μM) in the presence of increasing doses of FREG-(48–58). Spectra were obtained by exciting at 277 nm and collecting spectra between 300 and 400 nm. Data were corrected for the dilution (which never exceeded 5%), for the buffer, FREG-(48–58), and SCR contribution. Peak fluorescence at 310 nm, plotted as a function of FREG-(48–58)/FGF-2 molar ratio, shows a dose-dependent and saturable quench. *C* and *D*, SPR analysis showed that FGF-2 interaction with immobilized FGF-2 (*C*) or with immobilized heparin (*D*) reduces as a function of FREG-(48–58), while SCR shows no effect. *E*, FGF-2 interaction with FGF-R1 by SPR. Increasing concentrations of FREG-(48–58) (*1*, 0 ng/ml; *2*, 0.7 ng/ml; *3*, 2.1 ng/ml; *4*, 20 ng/ml; *5*, 180 ng/ml; *6*, 1.4 μg/ml; *7*, 14 μg/ml) dose-dependently inhibited FGF-2 interaction with immobilized FGF-R1, up to 40%, reaching the plateau at 180 ng/ml. A representative experiment is shown. This experiment was repeated three times with similar results.
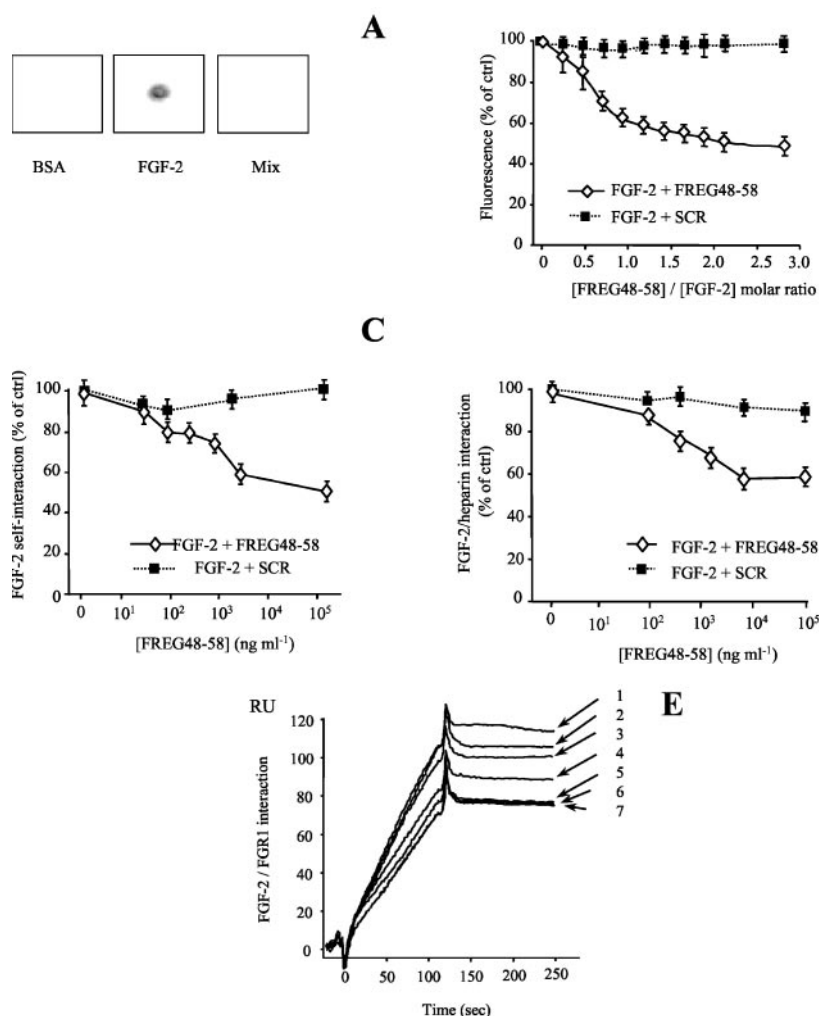
to allow detachment of the developing CAM. The window was sealed with a glass and the eggs returned to the incubator. On day 8, CAM was treated by applying the sponge as reported in the legend to Fig. 8. On day 12, blood vessels entering the sponge within the focal plane of the CAM were counted at ×50 magnification in a double-blind fashion under a Zeiss SR stereomicroscope (Zeiss) and photographed *in ovo* with the MC63 Camera System (Zeiss). Embryos and their membranes were fixed *in ovo* in Bouin's fluid. Sponges, the underlying and immediately adjacent portions of CAM were removed, embedded in paraffin, sectioned at 8 μm along a plane parallel to the CAM surface, and stained with a 0.5% aqueous solution of toluidine blue (Merck). The angiogenic response was assessed histologically by a planimetric method of "point counting" (48). The vascular density was indicated as the mean number of the occupied intersection points ± S.D.

Angiogenesis in Matrigel Plugs

The angiogenesis assay in Matrigel plugs was carried out as reported (31, 49). Briefly, Matrigel, a mixture of reconstituted basement membrane proteins (BD PharMingen, 600 μl) supplemented with FGF-2 (150 ng/ml) alone or in the presence of FREG-(48–58) or SCR (10 μg/ml), was injected subcutaneously in CD1 mice (female, 20 g body weight). Matrigel plugs were removed after 8 days and processed for histology analysis. Histologic sections (7 μm) were stained with Trichrome-Masson procedure (Bio-Optica). Vessels within the Matrigel were recognized by morphology and by the presence of red blood cells. Angiogenesis was evaluated blindly by two operators, by considering at least five different sections per Matrigel plug; each section was 100 μm from the next. The total number of neo-vessels in the whole Matrigel area was measured with an Axioplan microscope (Zeiss) and was expressed as the number of vessels/mm². When 2 vessels were cut longitudinally, as indicated by a long axis greater than 3-fold of the short axis, and were close to each other, they were counted as a single vessel. Ten animals were treated with FGF-2 alone, 14 with FGF-2 + FREG-(48–58), 10 with FGF-2 + SCR.

Statistics

Data were expressed as mean ± S.D. Student's two-tailed *t* test was performed, and $p \leq 0.01$ was considered statistically significant.

RESULTS

Analysis of FGF-2 Structure—Primary sequence analysis and three-dimensional structure evaluation were carried out on human FGF-2. A multiple sequence alignment was performed on the 23 members of the human fibroblast growth factor family (Fig. 1*A*). According to the consensus sequence at the 60% identity level, several residues are conserved within the family, while other regions show a high variability. In particular, the FGF-2 region 43–60 was found to be poorly conserved within the FGF family.

A docking simulation was carried out on two FGF-2 monomers (PDB code: 2BFH) leading to the prediction of a FGF-2 dimer (Fig. 1*B*); therefore regions at the dimer interface were predicted by solvent accessibility evaluation. Finally, on the high-resolution crystallographic model of the FGF-2/FGR1-heparin complex (PDB file: 1FQ9), regions interacting with the FGF-R1 were identified by solvent accessibility analysis (reported in the legend of Fig. 1*A*). According to all these analyses, the FGF-2 region 43–60 shows one of the lowest intrafamily identities and, at the same time, many residues of this segment were predicted to be involved in FGF-2 dimerization and were found to be involved in receptor binding. All together these observations suggested that this portion of FGF-2 may play a specific role in FGF-2 dimerization and receptor binding. To investigate this hypothesis, the follow-
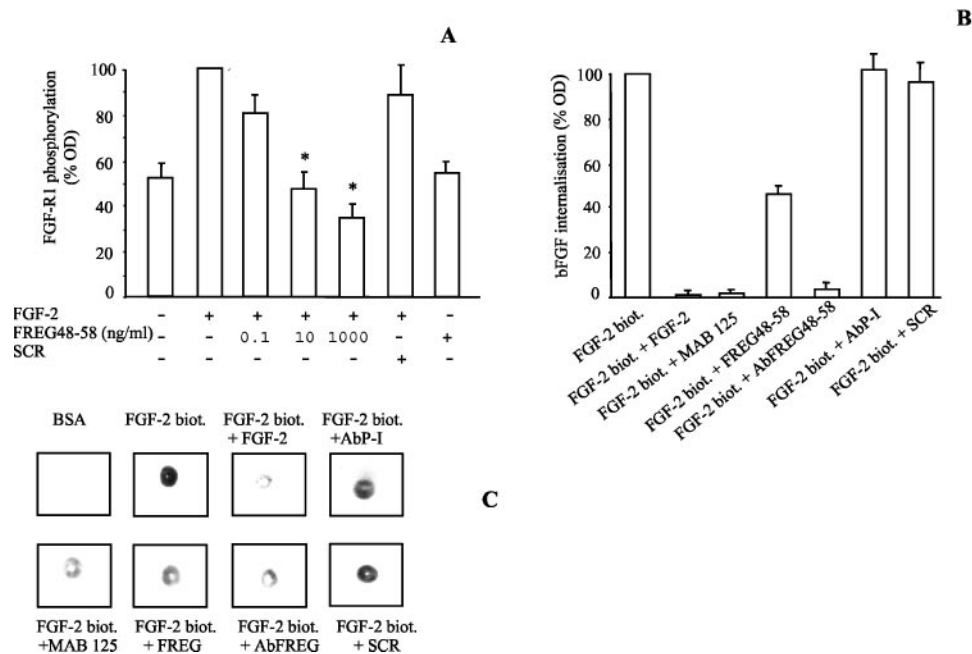
FIG. 5. **FREG-(48–58) effect on FGF-R1 phosphorylation and FGF-2 internalization.** *A*, FGF-R1 phosphorylation. FGF-R1 was immunoprecipitated and samples were subjected to electrophoresis and detected with an anti-phosphotyrosine antibody. FGF-2-induced FGF-R1 phosphorylation was dose-dependently inhibited in the presence of FREG-(48–58) (0.1–1000 ng/ml), while SCR was ineffective. Where not specified, peptides were used at a 10 ng/ml dose. Results represent the average of three experiments ± S.D. *Asterisk* indicates $p < 0.01$ *versus* FGF-2 alone. *B*, FGF-2 internalization. Membrane-bound biotinylated-FGF was discarded; internalized biotinylated-FGF-2 was spotted onto nitrocellulose and quantified. Internalization was significantly inhibited in the presence of an excess of unlabeled FGF-2, in the presence of the FGF-2 neutralizing monoclonal antibody mAb 125, and in the presence of FREG-(48–58) and of AbFREG48–58, while preimmune rabbit serum (AbP-I) and SCR were ineffective. Results represent the average of three experiments ± S.D. *C*, representative experiment of FGF-2 internalization.
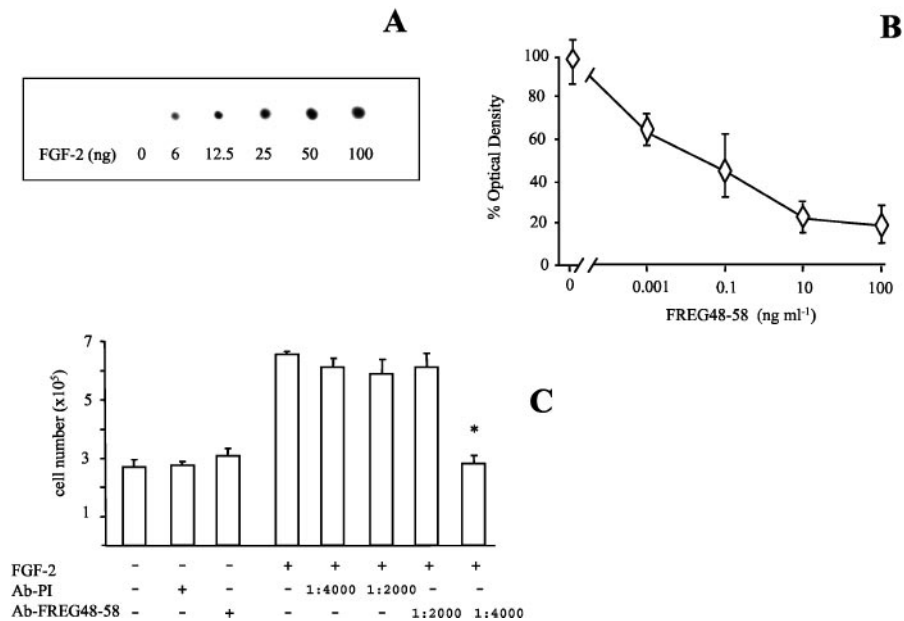

FIG. 6. **Investigating AbFREG48–58.** *A*, AbFREG48–58 interaction with immobilized FGF-2. Increasing quantities of FGF-2 were spotted onto nitrocellulose membrane (0, 6, 12.5, 25, 50, and 100 ng/spot, respectively); membrane was then incubated with AbFREG48–58 (1:200 in PBS), and bound antibody was revealed with anti-rabbit peroxidase-conjugated IgG and chemiluminescence. AbFREG48–58 recognized the immobilized FGF-2. This experiment was performed three times with similar results. *B*, FREG-(48–58) competition. Increasing quantities of FREG-(48–58) (up to 100 ng/ml) dose-dependently competed for the interaction between FGF-2 and AbFREG48–58, carried out as reported in *panel A*. *C*, FGF-2 induced BAEC proliferation at 48 h, in the presence of AbFREG48–58 (1:2000; 1:4000) or in the presence of preimmune rabbit serum (same dilutions). AbFREG48–58 (1:4000) significantly inhibited FGF-2-induced proliferation, while the control antibody was ineffective. The two antibodies did not modify cell number under basal conditions.

ing strategies were addressed: (i) one peptide derived from this region was designed, synthesized, and tested *in vitro* and *in vivo*, (ii) an antibody was developed against this peptide and tested in FGF-2-dependent *in vitro* assays, and (iii) histidine chemical modification was carried out because one of

the three FGF-2 histidines falls in the peptide region (*i.e.* His in position 50).

The secondary structure of residues 43–60 is characterized by a disordered segment, a short helix, a β-strand, and an additional short disordered segment. We selected a peptide
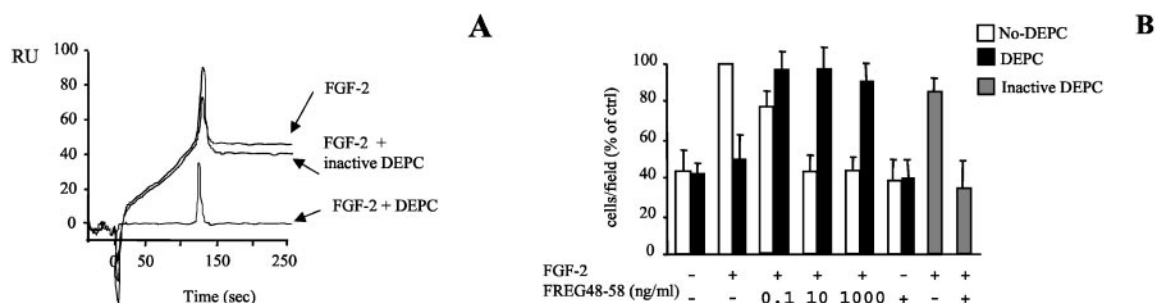
FIG. 7. **Histidines inactivation.** Histidines were chemically modified by incubating FGF-2 and FREG-(48–58) with DEPC. As a control, inactivated DEPC (*i.e.* DEPC in 100 mM Tris-HCl) was added. *A*, FGF-2 dimerization by SPR. Native FGF-2 interacted with immobilized FGF-2 reaching about 50 RU. In contrast, FGF-2 previously incubated with DEPC, entirely lost the ability to interact with immobilized FGF-2. Inactive DEPC did not modulate FGF-FGF interaction. A representative experiment is reported. This experiment was carried out three times, with similar results. *B*, BAEC migration induced by FGF-2, in the presence or in the absence of FREG-(48–58), previously treated or not treated with DEPC. FGF-2 entirely lost its ability to induce BAEC migration when histidines were modified; FREG-(48–58) (0.1–1000 ng/ml) dose-dependently inhibited BAEC migration, and at all tested doses the inhibitory effect was abolished after DEPC treatment. Where not specified, FREG-(48–58) was tested at 10 ng/ml. FGF-2 chemotactic activity was unaffected by incubation with inactive DEPC. Data are expressed as percent of the effect of FGF-2 alone ± S.D. In response to FGF-2, 31 ± 6 cells/field migrated.

including the short helix and the short β-strand, *i.e.* region 48–58 (DPHIKLQLQAE; FREG-(48–58)), to avoid excessive flexibility. FREG-(48–58) was therefore used in the following *in vitro* and *in vivo* analyses, and for rabbit immunization to raise a specific antibody.

Proliferation and Migration Assays—FGF-2-induced BAEC proliferation was evaluated at 48 h in the absence and presence of increasing FREG-(48–58) doses up to 1000 ng/ml (Fig. 2*A*). FREG-(48–58) showed a dose-dependent inhibitory activity and, at 10 ng/ml, lowered the FGF-2 mitogenic effect to the control level, while both scrambled peptides used as control (SCR) showed no activity. Therefore FREG-(48–58) and SCR at 10 ng/ml were used for the following *in vitro* experiments.

In time-course experiments FREG-(48–58) significantly inhibited FGF-2-induced proliferation, while SCR was ineffective (Fig. 2*B*). In the absence of FGF-2, FREG-(48–58) and SCR did not affect cell number, indicating that these compounds are not toxic on BAEC at the tested doses (not shown). Additional experiments showed that FREG-(48–58) markedly inhibited FGF-2-induced BAEC migration, while SCR was not effective (Fig. 3*A*). In contrast, EGF-, fibronectin-, and VEGF-induced migration were not impaired by FREG-(48–58) nor by SCR (Fig. 3, *B–D*, respectively), indicating that the FREG-(48–58) effect was FGF-2-specific.

FGF-2 Interaction with FREG-(48–58)—FREG-(48–58) was designed from the region at the predicted interface of the FGF-2 dimer. The hypothesis of a direct FREG-(48–58)/FGF-2 interaction was then tested in solid phase (overlay) assays and in liquid phase (fluorescence) experiments. Overlay assays showed that biotinylated FREG-(48–58) (200 μg/ml) specifically interacted with FGF-2 immobilized onto nitrocellulose (300 ng/spot), while it did not interact either with immobilized BSA or with a pool of immobilized purified proteins (molecular weight standards) (Fig. 4*A*).

Further studies indicated that FGF-2 fluorescence intensity at 310 nm was progressively quenched by increasing FREG-(48–58) concentration (Fig. 4*B*). The fluorescence quench reached a plateau around a FREG-(48–58)/FGF-2 molar ratio = 1, whereas no significant shift of the maximum fluorescence was observed. The quench reached 50% of the maximum effect (IC$_{50}$) at 1.33 ± 0.076 μM FREG-(48–58) concentration (*versus* FGF-2, 2 μM). The equilibrium dissociation constant (K_D), according to a non-linear least-square fitting, was equal to 579 ± 272 nM. Under similar experimental conditions SCR was ineffective.

Taken together these data indicate that a FREG-(48–58)/FGF-2 heterocomplex formation is observed in both solid phase and liquid phase conditions, with a K_D (in fluorescence studies) falling in the nanomolar range.

FGF-2 Interaction with FGF-2, with Heparin and with FGF-R1, in the Presence of FREG-(48–58)—FGF-2 dimerization is considered to be necessary for receptor binding and activation; therefore, a potential FREG-(48–58) interference with FGF-2/FGF-2 interaction was tested. SPR analyses showed that interaction of soluble FGF-2 with immobilized FGF-2 is inhibited by increasing doses of FREG-(48–58) up to about 50% (Fig. 4*C*). Further SPR experiments carried out on immobilized heparin showed that FREG-(48–58) markedly and dose-dependently reduced FGF-2 interaction with heparin (Fig. 4*D*). FREG-(48–58) IC$_{50}$ values in FGF-2 self-interaction and heparin-binding experiments were 820 ng/ml and 980 ng/ml, respectively. Additional SPR experiments showed that increasing FREG-(48–58) doses (from 0 to 14 μg/ml) inhibited up to 40% FGF-2 interaction with immobilized FGF-R1, reaching the plateau at 180 ng/ml (Fig. 4*E*).

FREG-(48–58) also inhibited FGF-2/FGF-2 interaction in overlay experiments, while the interaction of immobilized FGF-2 with a polyclonal anti-FGF-2 antibody was unaffected (data not shown). In all cases SCR was ineffective. Taken together, these data show that FREG-(48–58) strongly inhibits FGF-2 interaction with itself, with heparin, and with FGF-R1.

FGF-2 Receptor Phosphorylation and FGF-2 Internalization in the Presence of FREG-(48–58)—It was then tested whether the observed action of FREG-(48–58) would affect FGF-2-dependent receptor phosphorylation and FGF-2 internalization.

FGF-2-dependent phosphorylation of FGF-R1 in BAEC was markedly diminished by FREG-(48–58) (10 ng/ml), while SCR did not show any effect (Fig. 5*A*). Further, biotinylated FGF-2 internalization was measured in BAEC. A large excess of unlabeled FGF-2, as well as mAb 125, a FGF-2 neutralizing antibody (Chemicon), abolished FGF-2 internalization, as expected. Under such conditions, FREG-(48–58) significantly reduced FGF-2 internalization by about 50% while SCR was inactive. Quantification of this effect is reported in Fig. 5*B*, while Fig. 5*C* shows one representative experiment.

These results indicate that, in the presence of FREG-(48–58), FGF-2 internalization, which depends upon its binding to membrane-bound receptors, and FGF-R1 phosphorylation are markedly inhibited.

Developing the Anti-FREG-(48–58) Antibody (AbFREG48–58)—To further investigate the role of FGF-2 region 48–58, a rabbit polyclonal antibody was raised against FREG-(48–58) (AbFREG48–58) and was tested *in vitro*. It almost abolished FGF-2 internalization at a 1:200 dilution, and this effect was comparable to that of the commercially available neutralizing antibody mAb 125 used at a 1:500 dilution (Fig. 5, *B* and *C*). This finding supported the hypothesis that region 48–58

TABLE I
Chick embryo CAM-sponge assay: microvessel density

For histologic assessment, every third section of 30 serial slides from each specimen was analyzed under a 144-point mesh inserted into the eyepiece of the photomicroscope. The total number of intersection points occupied by transversally cut vessels (3–10 μm in diameter) were counted at $\times$250 magnification inside the sponge and at the boundary between the sponge and surrounding CAM mesenchyme in 6 randomly chosen microscopic fields per section and reported as mean $\pm$ S.D. Asterisks indicate statistically significant difference from FGF-2 ($p < 0.01$).

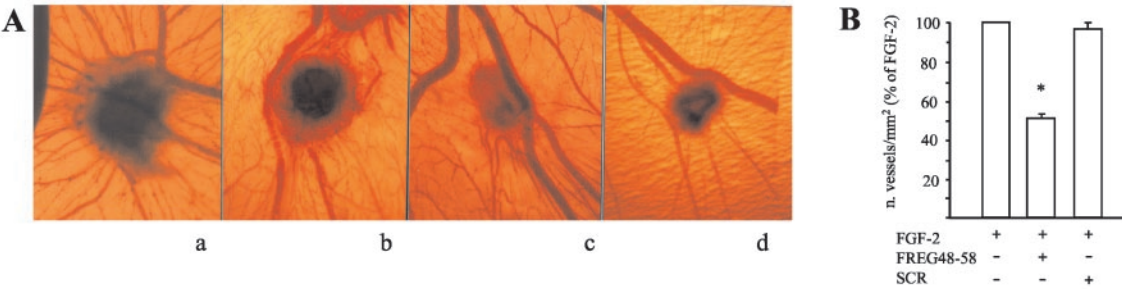| Sponge loaded with:	Number of specimens	Number of microvessels inside the sponge	Number of microvessels at the boundary
FGF-2	10	30 $\pm$ 5	40 $\pm$ 4*
FGF-2 + FREG-(48–58)	10	0	10 $\pm$ 3*
FREG-(48–58)	10	0	15 $\pm$ 4*
PBS	10	0	14 $\pm$ 3*

FIG. 8. **Angiogenesis assays in CAM and Matrigel.** *A*, on 8-day-old chick embryos, 1 mm^3 gelatin sponges (Gelfoam, Upjohn Company) loaded with 3 μl of PBS alone (*d*), or FREG-(48–58) alone (50 μg/ml) (*c*), or FGF-2 alone (500 ng) (*a*), or FGF-2 + FREG-(48–58) (500 ng and 50 μg, respectively) (*b*), were implanted; CAM were then analyzed at day 12. In *panel a* small blood vessels converge like spokes toward the sponge, while in *b*, *c*, and *d* there are very few small blood vessels around the sponge or converging toward it. Original magnification: $\times$50. *B*, quantification of angiogenesis in Matrigel plugs injected subcutaneously in CD1 mice, in the presence of FGF-2 alone (150 ng/ml), FGF-2 + FREG-(48–58) (150 ng/ml and 10 μg/ml, respectively), or FGF-2 + SCR (150 ng/ml and 10 μg/ml, respectively). FGF-2-induced angiogenesis was significantly inhibited by FREG-(48–58) ($p < 0.01$), while SCR was ineffective. Matrigel without FGF-2 presented 25 $\pm$ 8 vessels/mm^2. This number was subtracted from the other groups as background. Data are expressed as *% versus* control $\pm$ S.D. (100% = 250 $\pm$ 28 vessels/mm^2).

of FGF-2 may be functionally relevant. Furthermore, AbFREG48–58 recognized increasing doses of FGF-2 immobilized onto nitrocellulose (Fig. 6*A*), and FREG-(48–58) competed dose-dependently with this specific interaction (Fig. 6*B*). These results indicated that FREG-(48–58) represents an exposed epitope and may be a functionally relevant region of the whole FGF-2. This hypothesis was further confirmed in proliferation experiments in which AbFREG48–58 acted as neutralizing antibody by significantly reducing the FGF-2 mitogenic effect at 1:4000 dilution (Fig. 6*C*). These data indicate that AbFREG48–58 blocks FGF-2 internalization and the FGF-2 mitogenic effect, supporting the hypothesis that the region encompassing FREG-(48–58) is a crucial functional domain.

Histidine Residue Chemical Inactivation—Histidines are very reactive residues and often occupy functionally relevant sites in proteins. Human FGF-2 contains three histidines, His-16, His-35, and His-50, the latter falling within the FREG-(48–58) region. In order to test whether histidine residues play a role in FGF-2 activity, their direct and specific chemical inactivation was achieved by DEPC treatment. Interestingly, DEPC-treated FGF-2 was unable to interact with itself (Fig. 7*A*) and failed to induce BAEC chemotaxis (Fig. 7*B*). Further, inactivating FREG-(48–58) histidine by DEPC incubation, abolished the FREG-(48–58) ability to inhibit FGF-2-induced chemotaxis (Fig. 7*B*). Taken together these results show that histidines play a crucial functional role for FGF-2 activity *in vitro*, and indicate that the histidine present in FREG-(48–58) is essential for its biological effects.

In Vivo Angiogenesis Assays—In order to evaluate whether FREG-(48–58) modulates FGF-2 effects *in vivo*, two different assays were performed, *i.e.* the CAM assay and the Matrigel assay.

FREG-(48–58) Effect in the CAM Assay—Ten CAM per group were treated with PBS, FGF-2 alone, FREG-(48–58) alone, or FGF-2 + FREG-(48–58). Experiments were stopped at day 12

and examined macroscopically and histologically. FREG-(48–58) abolished the new vessel formation induced by FGF-2, either inside the sponge trabeculae or at the boundary between the sponge and the CAM mesenchyme. Quantification of the effect achieved by histologic examination and planimetric vessel counting is reported in Table I, and a representative experiment is reported in Fig. 8*A*.

FREG-(48–58) Effect in the Matrigel Assay—FGF-2-induced angiogenesis in Matrigel plugs injected subcutaneously in CD1 mice was also evaluated. Eight days after implant, Matrigel plugs were removed, histologically processed, and new blood vessel formation was measured. As shown in Fig. 8*B*, FREG-(48–58) significantly inhibited ($p < 0.01$) FGF-2-induced vessel formation by 49 $\pm$ 5%, while SCR was ineffective. Taken together, *in vivo* studies indicate that FREG-(48–58) markedly inhibits FGF-2-induced angiogenesis in two different *in vivo* assays.

DISCUSSION

FGF-2 dimerization is reported to be a necessary event for receptor dimerization and signaling activation; therefore, region(s) directly involved in FGF-2 dimerization may represent crucial site(s) controlling the whole FGF-2 activity. The dimer in the absence of heparin has not been crystallized for FGF-2 although it is known for FGF-9 (50). Conversely, complexes in the presence of heparin (but lacking a direct FGF-FGF interaction) have been crystallized for FGF-1 (51) and FGF-2 (20). These studies revealed different dimerization/oligomerization features for different members of the FGF family, likely due to the differences in the β1, β2, β9, and β10 loops, outside the β trefoil core (50). Different three-dimensional simulation-based studies predicted different organizations of the FGF-2 dimer in the absence of heparin (15–17) and indicated the theoretical possibility that FGF-2 monomers may interact and associate with different orientations. The dimer model predicted in this

study shows a high content of hydrophobic residues at the dimer interface (*i.e.* 41%), which might contribute stability to the predicted dimer. FREG-(48–58) was selected because its sequence is poorly conserved within the FGF family (Fig. 1*A*) (being specific for FGF-2, whereas other portions are conserved throughout the entire family), and because it falls at the predicted interface of the FGF-2 dimer. Further, it overlaps, or is close to, receptor- and heparin-binding residues. FREG-(48–58) strongly and specifically inhibited FGF-2 activity *in vitro* and markedly reduced FGF-2-induced new vessel formation *in vivo*. An FGF-2/FREG-(48–58) complex formation was observed and, likely as consequence of this, FGF-2 interaction with itself, with heparin, and with FGF-R1 was strongly reduced, as well as FGF-2-induced FGF-R1 phosphorylation and FGF-2 internalization. It is known that FGF-2 internalization follows its binding to either high affinity receptors or to heparan sulfate proteoglycans (51). Therefore, the observed FREG-(48–58)-induced inhibition of FGF-2 internalization (Fig. 5, *B* and *C*) may be due either to reduced interaction with high affinity receptors (Fig. 4*E*), to the inhibition of FGF-2 self-interaction (Fig. 4*C*), or to reduced interaction with heparan sulfate proteoglycans (Fig. 4*D*). In either case, the extensive inhibitory effect indicates that FREG-(48–58) may interfere with an early event essential for the receptor activation. FGF-2 region 48–58 may control an early event, likely dimerization, because the region 48–58 stays at the predicted FGF-2 dimerization interface, essential to activate FGF-2 signaling. In this case, the observed reduced heparin-binding, receptor binding, and receptor activation may be consequences of dimer formation inhibition. However, a direct effect of FREG-(48–58) on heparin binding and receptor binding cannot be ruled out at this stage. FREG-(48–58) may affect FGF-2 dimer formation by directly interacting with FGF-2 and masking the dimerization site, although presently we do not have a definitive indication of the site of interaction with FGF-2.

Alternative approaches confirmed that region 48–58 may be an FGF-2 crucial functional domain. In fact, the antibody raised against FREG-(48–58) recognized the whole FGF-2 and blocked FGF-2 internalization and its mitogenic effect, indicating that region 48–58 is a relevant epitope and that it may have a crucial functional role. Further, histidine modification abolished FGF-2 and FREG-(48–58) *in vitro* activities, indicating that histidines, and specifically His-50, play a crucial role for FGF-2 and FREG-(48–58) activity, respectively. Site-directed mutagenesis studies will further characterize active residues in this region.

Several endogenous factors control angiogenesis (31, 53–54) and a number of molecules inhibiting FGF-2 are currently being investigated (47, 55–62). Specifically inhibiting FGF-2-dimerization with FREG-(48–58) may represent a novel effective approach to modulate FGF-2 activity with potential therapeutic applications. To this respect, a biocomputing tool potentially helpful to investigate protein active sites has been recently made available (63) at crisceb.unina2.it/ASC/. In conclusion, results of the present study indicate a novel FGF-2 regulatory domain and identify a short peptide, which strongly inhibits FGF-2 activity both *in vitro* and *in vivo*. Further studies will be aimed at characterizing the potential therapeutic role of this peptide.

REFERENCES

1. Ornitz, D. M., and Itoh, N. (2001) *Genome Biol.* **2,** 3005.1–3005-12
2. Nugent, M. A., and Iozzo, R. V. (2000) *Int. J. Biochem. Cell Biol.* **32,** 115–120
3. Bikfalvi, A., Klein, S., Pintucci, G., and Rifkin D. B. (1997) *Endocr. Rev.* **18,** 26–45
4. Sommer, C., Sabel, M., Oertel, W. H., Kiessling, M., and Sautter, J. (1999) *Brain Res. Mol. Brain. Res.* **69,** 53–61
5. Cummings, B. J., Su, J. H., and Cotman, C. W. (1993) *Exp. Neurol.* **124,** 315–325
6. Barillari, G., Sgadari, C., Fiorelli, V., Samaniego, F., Colombini, S., Manzari, V., Modesti, A., Nair, B. C., Cafaro, A., Sturzl, M., and Ensoli, B. (1999) *Blood* **94,** 663–672
7. Wang, Y., and Becker, D. (1997) *Nat. Med.* **3,** 887–893
8. Chandler, L. A. (1999) *Int. J. Cancer* **81,** 451–458
9. Carmeliet, P., and Jain, R. K. (2000) *Nature* **407,** 249–257
10. Rutherford, C. Martin, W., Salame, M., Carrier, M., Anggard, E., and Ferns, G. (1997) *Atherosclerosis.* **130,** 45–51
11. Marler, J. J. Rubin, J. B., Trede, N. S., Connors, S., Grier, H., Upton, J., Mulliken, J. B., and Folkman, J. (2002) *Pediatrics,* **109,** E37
12. Compagni, A., Wilgenbus, P., Impagnatiello, M. A., Cotten, M., and Christofori, G. (2000) *Cancer Res.* **60,** 163–7169
13. Raballo, R., Rhee, J., Lyn-Cook, R., Leckman, J. F., Schwartz, M. L., and Vaccarino, F. M. (2000) *J. Neurosci.* **20,** 5012–5023
14. Dono, R., Texido, G., Dussel, R., Ehmke, H., and Zeller, R. (1998) *EMBO J.* **17,** 4213–4225
15. Safran, M., Eisenstein, M., Aviezer, D., and Yayon, A. (2000) *Biochem. J.* **345,** 107–113
16. Herr, A. B., Ornitz, D. M., Sasisekharan, R., Venkataraman, G., and Waksman, G. (1997) *J. Biol. Chem.* **272,** 16382–16389
17. Venkataraman, G., Sasisekharan, V., Herr, A. B., Ornitz, D. M., Waksman, G., Cooney, C. L., Langer, R., and Sasisekharan, R. (1996) *Proc. Natl. Acad. Sci. U. S. A.* **93,** 845–850
18. Plotnikov, A. N., Schlessinger, J., Hubbard, S. R., and Mohammadi, M. (1999) *Cell* **98,** 641–650
19. Plotnikov, A. N., Hubbard, S. R., Schlessinger, J., and Mohammadi, M. (2000) *Cell* **101,** 413–424
20. Schlessinger, J., Plotnikov, A. N., Ibrahimi, O. A., Eliseenkova, A. V., Yeh, B. K., Yayon, A., Linhardt, R. J., and Mohammadi, M. (2000) *Mol. Cell* **6,** 743–750
21. Padera, R., Venkataraman, G., Berry, D., Godavarti, R., and Sasisekharan, R. (1999) *FASEB J.* **13,** 1677–1687
22. Leenders, W. P., van Hinsbergh, V. W., van Genesen, S. T., Schoenmakers, J. G, van Zoelen, E. J., and Lubsen, N. H. (1997) *Growth Factors* **14,** 213–228
23. Arakawa, T., Holst, P., Narhi, L. O., Philo, J. S., Wen, J., Prestrelski, S. J., Zhu, X., Rees, D. C., and Fox, G. M. (1995) *J. Protein Chem.* **14,** 263–274
24. Li, L. Y., Safran, M., Aviezer, D., Bohlen, P., Seddon, A. P. and Yayon, A. (1994) *Biochemistry* **33,** 10999–11007
25. Baird, A., Schubert, D., Ling, N., and Guillemin, R. (1988) *Proc. Natl. Acad. Sci. U. S. A.* **85,** 2324–2328
26. Ray, J., Baird, A., and Gage, H. (1997) *Proc. Natl. Acad. Sci. U. S. A.* **94,** 7047–7052
27. Isacchi, A., Statuto, M., Chiesa, R., Bergonzoni, L., Rusnati, M., Sarmientos, P., Ragnotti, G., and Presta, M. (1991) *Proc. Natl. Acad. Sci. U. S. A.* **88,** 2628–2632
28. Presta, M., Gualandris, A., Urbinati, C., Rusnati, M., Coltrini, D., Isacchi, A., Caccia, P., and Bergonzoni, L. (1993) *Growth Factors* **9,** 269–278
29. Russo, K., Ragone, R., Facchiano, A. M., Capogrossi, M. C., and Facchiano, A. (2002) *J. Biol. Chem.* **277,** 1284–1291
30. Facchiano, A., De Marchis, F., Turchetti, E., Facchiano, F., Guglielmi, M., Denaro, A., Palumbo, R., Scoccianti, M., and Capogrossi, M. C. (2000) *J. Cell Sci.* **113,** 2855–2863
31. De Marchis, F., Ribatti, D., Giampietri, C., Lentini, A., Faraone, D., Scoccianti, M., Capogrossi, M. C., and Facchiano, A. (2002) *Blood* **99,** 2045–2053
32. Thompson, J. D., Higgins, D. G., and Gibson, T. J. (1994) *Nucleic Acids Res.* **22,** 4673–4680
33. Hubbard, S. J., Campbell, S. F., and Thornton, J. M. (1991) *J. Mol. Biol.* **220,** 507–530
34. Kabsch, W., and Sander, C. (1983) *Biopolymers* **22,** 2577–2637
35. Katchalski-Katzir, E., Shariv, I., Eisenstein, M., Friesem, A. A., Aflalo, C., and Vakser, I. A. (1992) *Proc. Natl. Acad. Sci. U. S. A.* **89,** 2195–2199
36. Vakser, I. A. (1995) *Protein Eng.* **8,** 371–377
37. Jing, N., Marchand, C., Liu, J., Mitra, R., Hogan, M. E., and Pommier, Y. (2000) *J. Biol. Chem.* **275,** 21460–21467
38. Bridges, A., Gruenke, L., Chang, Y. T., Vakser, I. A., Loew, G., and Waskell, L. (1998) *J. Biol. Chem.* **273,** 17036–17049
39. Vakser, I. A., Matar, O. G., and Lam, C. F. (1999) *Proc. Natl. Acad. Sci. U. S. A.* **96,** 8477–8482
40. Giampietri, C., Levrero, M., Felici, A., D'Alessio, A., Capogrossi, M. C., and Gaetano, C. (2000) *Cell Death Differ.* **7,** 292–301
41. Miles, E. W. (1977) *Methods Enzymol.* **47,** 431–442
42. Russo, K., Di Stasio, E., Macchia, G., Rosa, G., Brancaccio, A., and Petrucci, T. C. (2000) *Biochem. Biophys. Res. Commun.* **274,** 93–98
43. Vemuri, S. Beylin, I, Sluzky, V., Stratton, P., Eberlein, G., and Wang, Y. J. (1994) *J. Pharm. Pharmacol.* **46,** 481–486
44. Eftink, M. R. (1997) *Methods Enzymol.* **278,** 221–257
45. Goretzki, L., Burg, M. A., Grako, K. A., and Stallcup, W. B. (1999) *J. Biol. Chem.* **274,** 16831–16837
46. Bailly, S., Brand, C., Chambaz, E. M., and Feige, J. J. (1997) *J. Biol. Chem.* **272,** 16329–16334
47. Hagedorn, M., Zilberberg, L., Lozano, R. M., Cuevas, P., Canron, X., Redondo-Horcajo, M., Gimenez-Gallego, G., and Bikfalvi, A. (2001) *FASEB J.* **15,** 550–552
48. Ribatti, D., Gualandris, A., Bastaki, M., Vacca, A., Iurlaro, M., Roncali, L., and Presta, M. (1997) *J. Vasc. Res.* **34,** 455–463
49. Facchiano, F., Lentini, A., Fogliano, V., Mancarella, S., Rossi, C., Facchiano, A., and Capogrossi, M. C. (2002) *Am. J. Pathology* **161,** 531–541
50. Plotnikov, A. N., Eliseenkova, A. V., Ibrahimi, O. A., Shriver, Z., Sasisekharan,

R., Lemmon, M. A., and Mohammadi, M. (2001) *J. Biol. Chem.* **276,** 4322–4329

51. Di Gabriele, A. D., Lax, I., Chen, D. I., Svahn, C. M., Jaye, M., Schlessinger, J., and Hendrickson, W. A. (1998) *Nature* **393,** 812–817
52. Gleizes, P. E., Noaillac-Depeyre, J., Amalric, F., and Gas, N. (1995) *Eur. J. Cell Biol.* **66,** 47–59
53. Cao, Y. (2001) *Int. J. Biochem. Cell Biol.* **33,** 357–369
54. Ruhrberg, C. (2001) *J. Cell Sci.* **114,** 3215–3216
55. Griffin, R. J., Williams, B. W., Wild, R. Cherrington, J. M., Park, H., and Song, C. W. (2002) *Cancer Res.* **62,** 1702–1706
56. Ciardiello, F. Caputo, R., Bianco, R., Damiano, V., Fontanini, G., Cuccato, S., De Placido, S., Bianco, A. R., and Tortora, G. (2001) *Clin. Cancer Res.* **7,** 1459–1465
57. Song, S., Wientjes, M. G., Gan, Y., and Au, J. L. (2000) *Proc. Natl. Acad. Sci. U. S. A.*, **97,** 8658–8663
58. Thompson, A. M., Connolly, C. J., Hamby, J. M., Boushelle, S., Hartl, B. G., Amar, A. M., Kraker, A. J., Driscoll, D. L., Steinkampf, R. W., Patmore, S. J., Vincent, P. W., Roberts, B. J., Elliott, W. L., Klohs, W., Leopold, W. R., Showalter, H. D., and Denny, W. A. (2000) *J. Med. Chem.* **43,** 4200–4211
59. Skaper, S. D., Kee, W. J., Facci, L., Macdonald, G., Doherty, P., and Walsh, F. S. (2000) *J. Neurochem.* **75,** 1520–1527
60. Aviezer, D., Cotton, S., David, M., Segev, A., Khaselev, N., Galili, N., Gross, Z., and Yayon, A. (2000) *Cancer Res.* **60,** 2973–2980
61. Perollet, C., Han, Z. C., Savona, C., Caen, J. P., and Bikfalvi, A. (1998) *Blood* **91,** 3289–3299
62. Mohammadi, M., Froum, S., Hamby, J. M., Schroeder, M. C., Panek, R. L., Lu, G. H., Eliseenkova, A. V., Green, D., Schlessinger, J., and Hubbard, S. R. (1998) *EMBO J.* **17,** 5896–5904
63. Facchiano, A. M., Facchiano, A., and Facchiano, F. (2003) *Nucleic Acid Res.* **31,** 379–382

Identification of a Novel Domain of Fibroblast Growth Factor 2 Controlling Its Angiogenic Properties

Antonio Facchiano, Katia Russo, Angelo M. Facchiano, Francesco De Marchis, Francesco Facchiano, Domenico Ribatti, Maria S. Aguzzi and Maurizio C. Capogrossi

Access the most updated version of this article at doi: 10.1074/jbc.M209936200

Alerts:
- When this article is cited
- When a correction for this article is posted

Click here to choose from all of JBC's e-mail alerts

This article cites 63 references, 25 of which can be accessed free at
http://www.jbc.org/content/278/10/8751.full.html#ref-list-1